SEISMIC DATA RECONSTRUCTION COMBINING DISCRETE COSINE TRANSFORM AND SHEARLET TRANSFORM

HAIYANG YAN[1,2,3,4], HUI ZHOU[1,2,3], HAIBO LIU[4], ZHAOHONG XU[4], ZANDONG SUN[4], ZHAO LIU[4] and MINGKUN ZHANG[1,2,3]

[1] *State Key Laboratory of Petroleum Resources and Prospecting, Beijing 100029, P.R. China. huizhou@cup.edu.cn*
[2] *CNPC Key Lab of Geophysical Exploration, Beijing, 100029, P.R. China.*
[3] *China University of Petroleum-Beijing, Beijing 102249, P.R. China.*
[4] *BGP Offshore, CNPC, Tianjin 300457, P.R. China.*

(Received February 1, 2023; accepted May 6, 2023)

ABSTRACT

Yan, H.Y., Zhou, H., Liu, H.B., Xu, Z.H., Sun, Z.D., Liu, Z. and Zhang, M.K., 2023. Seismic data reconstruction combining discrete cosine transform and shearlet transform. *Journal of Seismic Exploration*, 32: 301-314.

The irregularity of seismic data caused by field acquisition affects the imaging quality of subsequent seismic data processing. The reconstruction method based on compressed sensing theory can effectively restore seismic data. The aliasing caused by randomly missing seismic traces is distributed as white noise, and the effective signals are concentrated in the sparse domain. This paper transforms the seismic data reconstruction in the *t-x* domain into the random noise suppression problem in the discrete cosine transform (DCT) domain. The DCT is a global transform, which transforms the discontinuous *t-x* data into the continuous DCT data. We do multi-scale directional shearlet transform on the data in the DCT domain and eliminate the aliasing in the DCT domain through iterative inversion. The shearlet transform after the DCT can be used as a new sparse basis transform. The reconstruction experiments show that the reconstruction accuracy in the DCT+shearlet domain is higher than that in the shearlet domain.

KEY WORDS: shearlet transform, DCT, compressed sensing, seismic data reconstruction.

0963-0651/23/$5.00

INTRODUCTION

The lack of seismic data caused by field acquisition environment or economic acquisition affects the subsequent seismic processing and migration imaging. In theory, the data reconstruction method based on compressed sensing can break through the limitation of Nyquist frequency and recover the missing seismic data in the full frequency band. Compressed sensing data reconstruction mainly includes sparse sampling, sparse basis transform, and reconstruction methods. Seismic data in the *t-x* domain is not sparse, but it can meet sparse requirements through mathematical transformation. The coefficients corresponding to the effective signals are distributed intensively and relatively large, while the coefficients corresponding to the aliasing are very small. Fourier transform is applied to data reconstruction (Zhang et al., 2013; Gao et al., 2010; Zwartjes et al., 2007; Yang et al., 2013). Since the length of Fourier basis functions is very long, the Fourier transform does not contain any local information. The reconstruction effect based on the Fourier transform needs to be improved. Wavelet transform is a multi-scale transform, which can extract local spectral and temporal information simultaneously (Pawelec et al., 2021), but it has the disadvantage of poor directionality. To overcome the missing directional selectivity of conventional discrete wavelet transform (DWT), curvelet transform has been applied in compressed sensing seismic data reconstruction (Yang et al., 2012; Zhang et al., 2019; Zhang et al., 2015; Yang et al., 2012; Zhang et al., 2019). Radon and curvelet transform are combined to improve the sparsity of the data, and the reconstruction effect is further improved (Wang et al., 2019; Gong et al., 2018). The Curvelet Transform is not singly generated. Its construction involves rotations, which prevents a direct transition from the continuum to the digital setting. To overcome the main drawbacks of the curvelet representation, shearlet transform is proposed. It is well applied in microseismic data denoising (Tang et al., 2018) and seismic data reconstruction (Zhang et al., 2019; Liu et al., 2018).

In this paper, we transform the seismic data reconstruction problem in the *t-x* domain into a random noise suppression problem in the DCT domain. First, the missing seismic data is transformed by the DCT, then the DCT data is transformed by the shearlet transform. The aliasing caused by the missing seismic traces in the DCT domain is eliminated by iterative inversion to realize seismic reconstruction. Different from the seismic data reconstruction using a dictionary combination of Shearlet and DCT under the MCA (morphological component analysis) framework (Wang et al.,2021), the signal is formed by the linear combination of multiple different morphological components, and seismic data reconstruction is performed by using different sparse dictionary combination. The DCT +shearlet transform adopted in this paper can be regarded as a new sparse basis transform, which does not need to solve each morphological component iteratively. Different from the conventional reconstruction of missing seismic data in the *t-x* domain, we transform the data reconstruction problem in the discontinuous *t-x* domain into the random noise suppression problem in the continuous DCT domain. The synthetic and field data examples show that the

reconstruction effect in the DCT+shearlet domain is better than that in the shearlet domain.

THEORY

Compressed sensing reconstruction algorithms

Considering the shortcomings of the traditional sampling theorem and the sparse characteristics of the signal, Candès et al. (2006) and Donoho (2006) proposed the compressed sensing theory. Seismic data reconstruction based on compressed sensing can be expressed as solving equations:

$$\mathbf{d} = \mathbf{mf} \quad , \tag{1}$$

where $\mathbf{f} \in R^{p}$ is the data to be recovered. $\mathbf{d} \in R^{q}$ is the acquired data. $\mathbf{M} \in R^{pxq}$ is the sampling diagonal matrix, and its elements on the diagonal correspond to **d**. When **d** is not missing, the element on the corresponding sampling diagonal is 1, otherwise it is 0.

In this paper, the DCT+shearlet transform is used to achieve sparser representations of the seismic data, and the problem of discontinuous seismic data reconstruction in the *t-x* domain is transformed into the problem of random noise suppression in the continuous DCT domain. The sparse basis is the shearlet basis function

$$\mathbf{x} = \varphi\psi\mathbf{f} \quad ,, \tag{2}$$

where ψ is the forward DCT, and φ is the forward shearlet transform, **x** is the result of the DCT+shearlet transform of **f**.

Insertion of (2) into (1) yields

$$\mathbf{d} = \mathbf{M}\psi^{-1}\varphi^{-1}\mathbf{x} = \theta\mathbf{x} \quad , \tag{3}$$

where ψ^{-1} is the inverse DCT, φ^{-1} is the inverse shearlet transform, and $\theta = \mathbf{M}\psi^{-1}\varphi^{-1}$ is the sensing matrix.

The problem of the seismic data reconstruction can be expressed as:

$$\tilde{\mathbf{x}} = \min \left\| \mathbf{x} \right\|_0 \qquad \text{s.t.} \quad \mathbf{d} = \theta\mathbf{x} \tag{4}$$

Under certain conditions, the L0-norm problem can be transformed into the L1-norm problem.

$$\tilde{\mathbf{x}} = \min \left\| \mathbf{x} \right\|_1 \qquad \text{s.t.} \quad \mathbf{d} = \theta\mathbf{x} \tag{5}$$

Set ε as reconstruction error, eq. (5) can be written as:

$$\tilde{\mathbf{x}}=\min\|\mathbf{x}\|_1 \quad \text{s.t.} \quad \|\mathbf{d}-\theta\mathbf{x}\|_1<\varepsilon \quad . \tag{6}$$

We use the POCS method (Zhang et al., 2013; Gao et al., 2010; Yang et al., 2012; Zhang et al., 2019; Zhang et al., 2015;) for the seismic data reconstruction in the DCT+shearlet domain.

$$\mathbf{d}_{k+1}=\psi^{-1}\varphi^{-1}T_{\lambda_k}\left(\varphi\psi\bar{\mathbf{d}}_k\right) \tag{7}$$

$$\bar{\mathbf{d}}_{k+1}=\mathbf{d}^{\text{obs}}+\left(\mathbf{I}-\mathbf{M}\right)\mathbf{d}_{k+1} \tag{8}$$

where $\boldsymbol{d}^{\text{obs}}$ is observed data. T_{λ_k} is a soft threshold function. λ_k is a threshold. k *i*s the number of iterations. $\boldsymbol{d}_{k+1}$ is updated data for iterations k+1. $\bar{\boldsymbol{d}}_{k+1}$ is the result of reinserting $\boldsymbol{d}^{\text{obs}}$ into $\boldsymbol{d}_{k+1}$. $\bar{\boldsymbol{d}}_1$ is equal to $\boldsymbol{d}^{\text{obs}}$. $\mathbf{I}$ is unit matrix. Among various interpolation methods, POCS is widely used because of its simple implementation and strong robustness.

DCT+shearlet transform

The DCT is a transform related to the Fourier transform. It is similar to discrete Fourier transform, DCT is a global transform. The coefficient distribution in the DCT domain is relatively concentrated in the low-frequency band. In 2D case, the DCT is given by:

$$F(u,v)=a_u a_v\sum_{x=1}^{J}\sum_{y=1}^{L}f(x,y)\cos\frac{(2x+1)u\pi}{2J}\cos\frac{(2y+1)v\pi}{2L} \tag{9}$$

where

$$a_u=\begin{cases}\dfrac{1}{\sqrt{J}}, u=0\\ \dfrac{2}{\sqrt{J}}, u\neq 0\end{cases}, a_v=\begin{cases}\dfrac{1}{\sqrt{L}}, v=0\\ \dfrac{2}{\sqrt{L}}, v\neq 0\end{cases} \tag{10}$$

with x and $u=1,2,...,J$, y and $v=1,2,...,L$.

Shearlet transform (Guo et al., 2007; Easley et al., 2008; Guo et al., 2013) can effectively represent anisotropic characteristics of seismic data. The rotation model of curvelet transform is replaced by shear mode.In 2D case, for any square-integrable function $b(t)$, the shearlet transform is given by:

$$\mathrm{SH}_{\phi} b(j,l,k) = \left\langle b, \phi_{j,l,k} \right\rangle \quad , \tag{11}$$

where

$$\phi_{j,l,k}(\mathbf{t}) = \left|\det \mathbf{A}\right|^{-\frac{1}{2}} \phi\left[\mathbf{B}^{-1}\mathbf{A}^{-1}(\mathbf{t}-\mathbf{k})\right] \quad , \tag{12}$$

where $j \in \mathrm{R}^{+}, l \in \mathrm{R}, \mathbf{k} \in \mathrm{R}^{2}$, $\mathbf{A}$ is the anisotropic expansion matrix. $\mathbf{B}$ is the shear matrix, and both $\mathbf{A}$ and $\mathbf{B}$ are second-order reversible matrices. j is the scale parameter. l is the shear parameter, and k is the translation parameter.

To compare the effects of the shearlet transform and the DCT+shearlet transform, we use a 1-scale shearlet decomposition for simplification. A synthetic shot gather of the Marmousi model is used in this study. The shot has 512 receivers with a 10 m interval and 1 ms sampling. The shot is decomposed into 1 low-frequency subband without directional characteristics and 8 high-frequency subbands with directional characteristics. The energy of 9 subbands in the DCT+shearlet domain is more balanced than that in the shearlet domain. Fig. 1 shows the shot and its 2D-DCT, and Fig. 2 shows 9 coefficients of the shearlet decomposition. The energy of the low-frequency subband shown in Fig 2 (e) occupies 97.13% of that of the 9 subbands shown in Fig. 2. Fig. 3 shows 9 subbands of the DCT+shearlet decomposition. The energy of the low-frequency subband shown in Fig. 3(e) occupies 75.78% of that of the 9 subbands shown in Fig.3. Table 1 is the energy ratio comparison of different subbands in the shearlet and the DCT+shearlet domain. The energy of subbands in the DCT+shearlet domain is more balanced than that in the shearlet domain, which is more conducive to the data reconstruction based on iterative shrinkage-thresholding inversion.

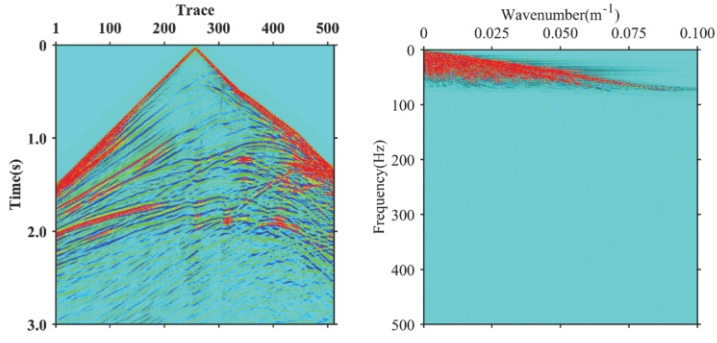

(a) (b)

Fig. 1. A shot gather of the Marmousi model (a) and its 2D-DCT data (b).

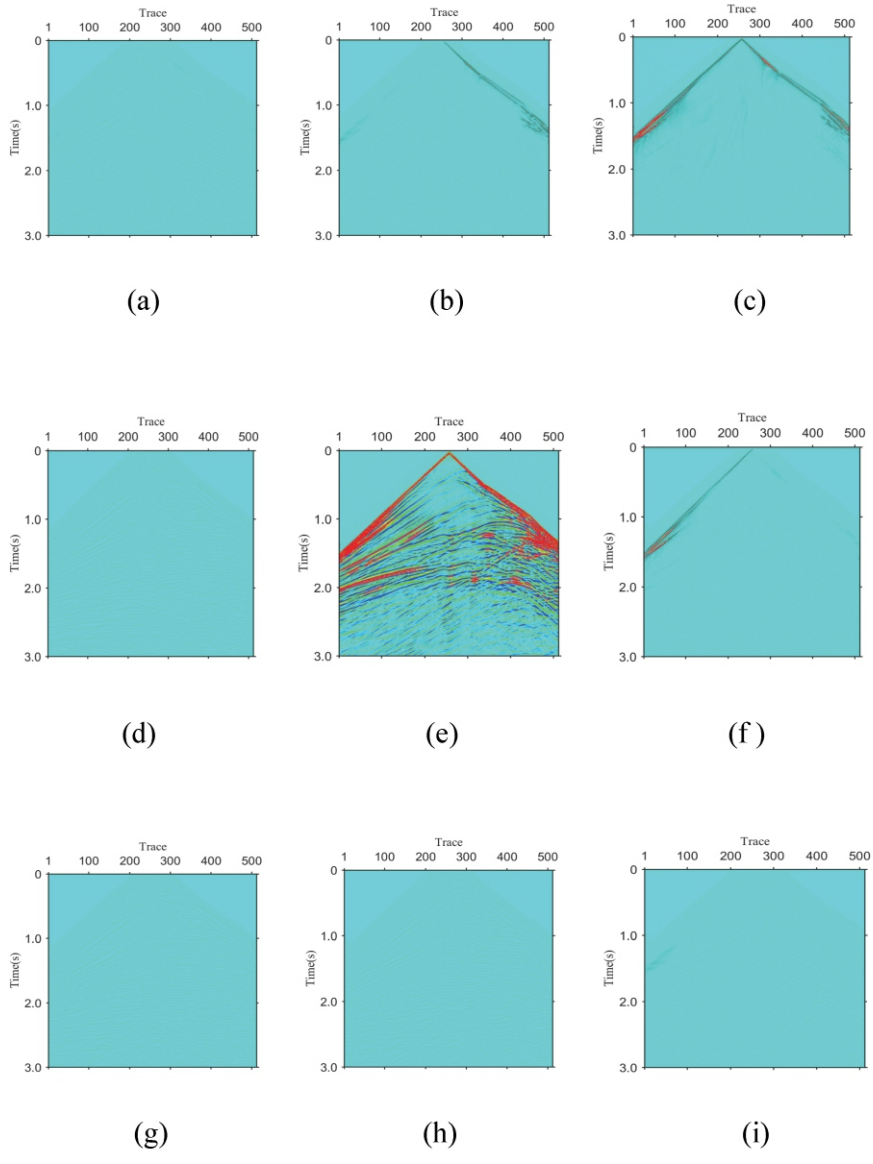

Fig. 2. Nine subbands of 1-scale shearlet transform decomposition.
(a)-(d) and (f)-(i) Eight high-frequency subbands, and (e) the low-frequency subband.

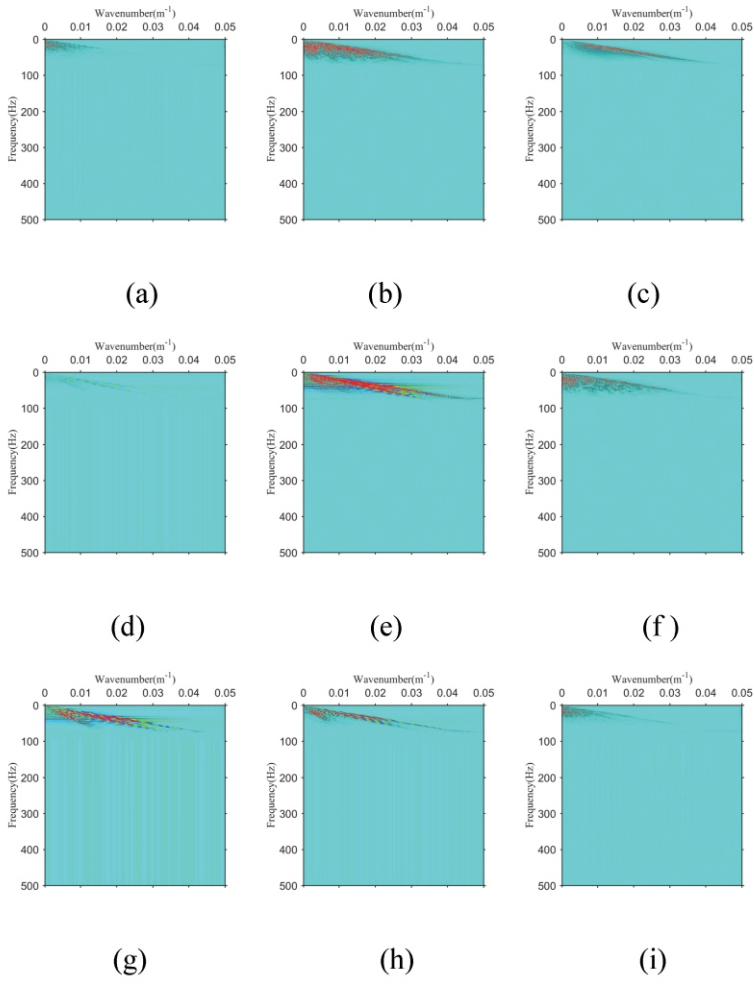

Fig. 3. Nine subbands of 1-scale DCT+shearlet transform decomposition.
(a)-(d) and (f)-(i) Eight high-frequency subbands, and (e) the low-frequency subband.

Table 1. Energy ratio comparison of different subbands in the shearlet and the DCT+shearlet domain.

Subbands	shearlet(%)	DCT+shearlet(%)
a	0.0027	0.4500
b	0.1700	7.3100
c	2.1900	2.3800
d	0.4900	2.5700
e	0.0059	0.5600
f	0.0000	2.7200
g	0.0000	8.1500
h	0.0000	0.0700
i	97.1300	75.7800

SYNTHETIC TEST

To evaluate the reconstruction quality, signal-to-noise ratio (SNR) is defined as follows:

$$SNR = 10\log_{10}\left(\left\|\mathbf{x}\right\|^2 \Big/ \left\|\mathbf{x}^* - \mathbf{x}\right\|^2\right) \quad , \tag{13}$$

where $\mathbf{x}$ is the original data and $\mathbf{x}^*$ is the reconstructed data.

To compare the data reconstruction effect in the shearlet domain and the DCT+shearlet domain, the synthetic shot shown in Fig. 1 (a) is used in this study. The shot is 40% randomly decimated shown in Fig. 4 (a). Fig. 4 (b) is 2D-DCT of Fig. 4 (a). The data in the DCT domain [Fig. 4 (b)] is more sparse than that in the *t*-*x* domain [Fig. 4 (a)]. When seismic data is missing, it's discontinuous in the *t*-*x* domain, but it's continuous in the DCT domain with spatial aliasing caused by the missing seismic data.

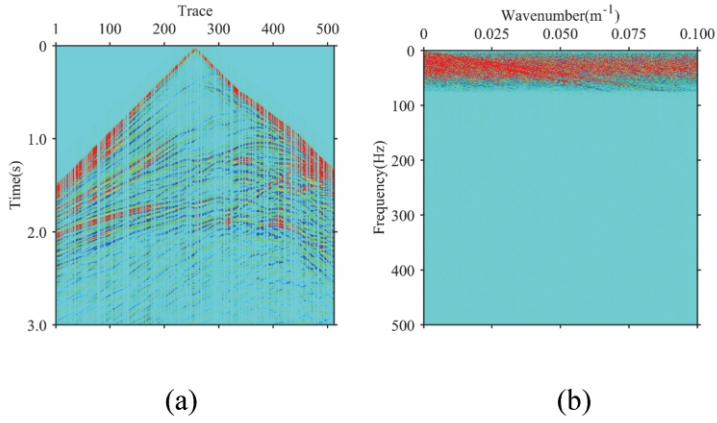

Fig. 4. The shot with 40% randomly decimated (a) and its 2D-DCT(b).

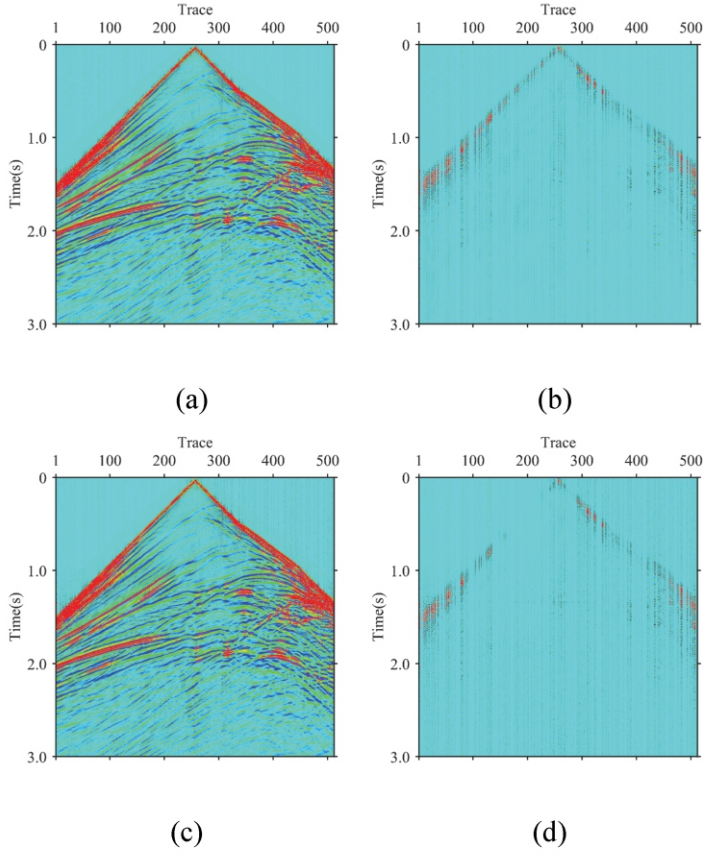

Fig. 5. Comparison of reconstruction results of Fig. 4 (a) in different sparse domains. (a) Reconstructed result in the shearlet domain, (b) difference between Fig. 5 (a) and Fig. 1(a), (c) reconstructed result in the DCT+shearlet domain, (d) difference between Fig. 5 (c) and Fig. 1 (a).

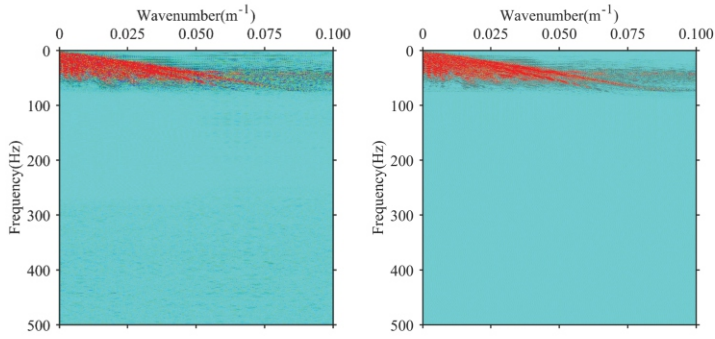

(a) (b)

Fig. 6 DCT data comparison (a) DCT of Fig 5 (a) reconstructed in shearlet domain, (b) DCT of Fig 5 (c) reconstructed in DCT+shearlet domain.

Fig. 5 shows the reconstruction results of Fig. 4 (a) in different sparse domains. The reconstruction error in the shearlet domain [Fig. 5 (b)] is greater than that in the DCT+shearlet domain [Fig. 5 (d)]. The SNR of seismic data reconstruction in the shearlet domain [Fig. 5 (a)] is 15.42 and that in the DCT+shearlet domain [Fig. 5 (c)] is 17.01. Fig. 6 shows the DCT data comparison of seismic data recovered from different sparse domains. The spatial aliasing in the DCT domain is well suppressed after compressed sensing reconstruction. The dct of seismic data recovered in DCT+shearlet domain [Fig. 6 (a)] is closer to the original DCT data [Fig. 1 (b)] than that in shearlet domain [Fig. 6 (b)].

FIELD DATA

To verify this method's effectiveness and practicability, we conducted trial processing on a marine shot [Fig. 7 (a)]. The shot has 380 receivers with a 6.65 m interval and 1 ms sampling. Fig 7 (b) is the 2D-DCT of Fig 7 (a). The shot is 30% randomly decimated [Fig. 7 (c)]. Fig. 7 (d) is the 2D-DCT of Fig. 7 (c). Fig. 8 shows the reconstruction results of Fig. 7 (c). The reconstruction error in the shearlet domain [Fig. 8 (b)] is evidently greater than that in the DCT+shearlet domain [Fig. 8 (d)]. The SNR of reconstructed data in the shearlet domain [Fig. 8 (a)] is 5.46 and that in the DCT+shearlet domain [Fig. 8 (c)] is 12.32. The reconstruction effect in the DCT+shearlet domain is better than that in the shearlet domain.

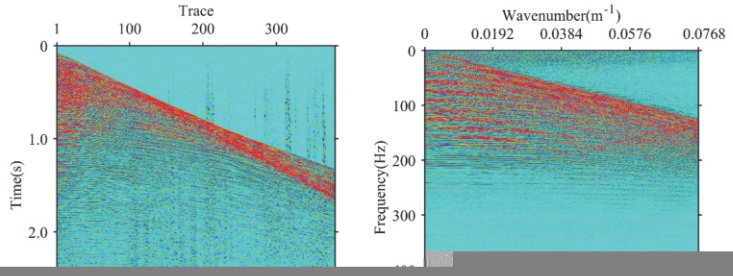
Trace
1
100
200
300
0
1.0
2.0
Time(s)
Wavenumber(m-1)
0
0.0192
0.0384
0.0576
0.0768
0
100
200
300
Frequency(Hz)

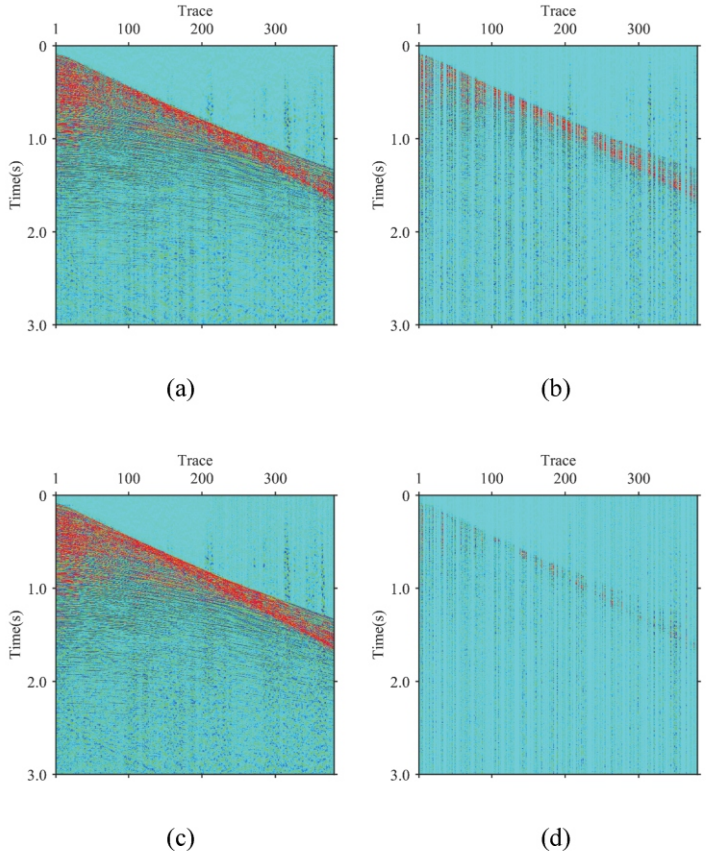

Fig. 8. Comparison of reconstruction results of Fig. 7 (a) in different sparse domains. (a) Reconstructed result in the shearlet domain, (b) difference between Fig. 8 (a) and Fig. 7 (a), (c) reconstructed result in the DCT+shearlet domain, (d) difference between Fig. 8 (c) and Fig. 7 (a).

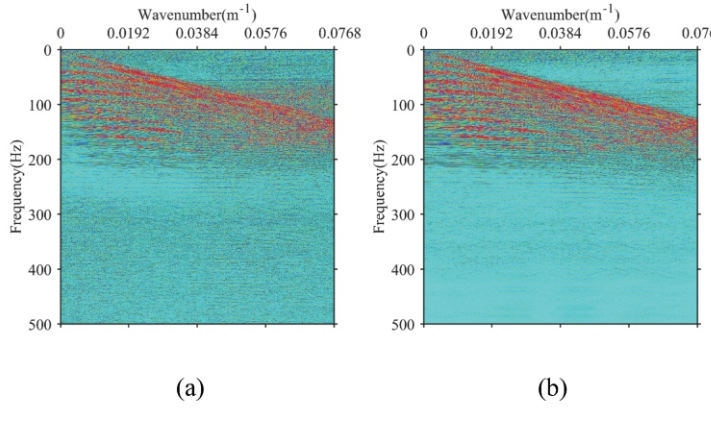

Fig. 9. DCT data comparison (a) DCT of Fig. 8 (a) reconstructed in shearlet domain, (b) DCT of Fig. 8 (c) reconstructed in DCT+shearlet domain.

Fig. 9 shows the DCT data comparison of seismic data recovered from different sparse domains. The spatial aliasing in the DCT domain is well suppressed after compressed sensing reconstruction. The DCT of seismic data recovered in DCT+shearlet domain [Fig. 9 (a)] is closer to the original DCT data [Fig. 7 (b)] than that in shearlet domain [Fig. 9 (b)].

CONCLUSION

In this study, the DCT+shearlet transform was proposed as a new sparse basis transform. The data reconstruction problem in the discontinuous t-x domain was transformed into the random noise suppression problem in the continuous DCT domain. Experiments show that the reconstruction result in the DCT+shearlet domain is better than that in the shearlet domain.

The DCT+shearlet transform can be applied to the suppression of seismic random noise and deblending of simultaneous-source. Similar to DCT+shearlet transform, we can perform new transforms, such as DCT+wavelet, DCT+curvelet, DCT+NSST (nondownsampling shearlet transform), etc.

ACKNOWLEDGEMENTS

This work was supported in part by the National Natural Science Foundation of China under Grant U19B6003-04.

REFERENCES

Candès, E.J., Romberg, J. and Tao, T., 2006. Robust uncertainty principles: exact signal reconstruction from highly incomplete frequency information. IEEE Transact. Inform. Theory, 52: 489-509.

Donoho, D.L., 2006. Compressed sensing. IEEE Transact. Inform. Theory, 52: 1289-1306.

Easley, G., Labate, D. and Lim, W.-Q., 2008. Sparse directional image representations using the discrete shearlet transform. Appl. Computat. Harmon. Analys., 25: 25-46.

Gao, J.J., Chen, X.H., Li, J.Y., Liu, G.C. and Ma, J., 2010. Irregular seismic data reconstruction based on exponential threshold model of POCS method. Appl. Geophys., 7: 229-238.

Gong, X., Wang, S. and Du, L. 2018. Seismic data reconstruction using a sparsity-promoting apex shifted hyperbolic Radon-curvelet transform. Stud. Geophys. Geod, 62: 450-465.

Guo, K. and Labate, D., 2007. Optimally sparse multidimensional representation using shearlets. SIAM J. Math. Anal., 39: 298-318.

Guo, K. and Labate, D., 2013. The Construction of Smooth Parseval Frames of Shearlets. Math. Model. Nat. Phenom., 8: 82-105.

Liu, C., Wang, D., Sun, J. and Wang, T., 2018. Crossline-direction reconstruction of multi-component seismic data with shearlet sparsity constraint. J. Geophys. Engin., 15:1929-1942.

Pawelec, I., Wakin, M. and Sava, P., 2021. Missing trace reconstruction for 2D land seismic data with randomized sparse sampling. Geophysics., 86(3): 25-36.

Tang, N., Zhao, X., Li, Y. and Zhu, D., 2018. Adaptive threshold shearlet transform for surface microseismic data denoising. J. Appl. Geophys.,153: 64-74.

Titova, A., Wakin, M.B. and Tura, A., 2021. Empirical analysis of compressive sensing reconstruction using the curvelet transform: SEAM Barrett model. First International Meeting for Applied Geoscience & Energy, Denver, CO.

Wang, D., Zhang, K., Li, Z., Xu, X. and Zhang, Y., 2021. Seismic data reconstruction using Shearlet and DCT dictionary combination. First International Meeting for Applied Geoscience & Energy, Denver, CO.

Wang, H., Tao, C., Chen, S., Wu, Z., Du, Y., Zhou, J., Qiu, L., Shen, H., Xu, W. and Liu, Y., 2019. High-precision seismic data reconstruction with multi-domain sparsity constraints based on curvelet and high-resolution Radon transforms. J. Appl. Geophys., 162: 128-137.

Yang, P. , Gao, J. and Chen, W., 2013. Irregularly sampled seismic data interpolation using iterative half thresholding regularization. IEEE Internat. Conf. Acoustics, Speech and Signal Process. (ICASSP): 5820-5824,

Yang, P., Gao, J. and Chen, W., 2012. Curvelet-based POCS interpolation of nonuniformly sampled seismic records. J. Appl. Geophys., 79: 90-99.

Zhang, H., Chen, X.H. and Wu, X.M., 2013. Seismic data reconstruction based on CS and Fourier theory. Appl. Geophys., 10: 170-180.

Zhang, H., Diao, S., Chen, W., Huang, G., Li, H. and. Bai M, 2019. Curvelet reconstruction of non-uniformly sampled seismic data using the linearized Bregman method. Geophys. Prosp., 67: 1201-1218.

Zhang, H., Diao, S., Chen, W., Huang, G., Li, H. and Bai, M., 2019. Curvelet reconstruction of non-uniformly sampled seismic data using the linearized Bregman method. Geophys. Prosp., 67: 1201-1218.

Zhang, H., Chen, X. and Li, H., 2015. 3D seismic data reconstruction based on complex-valued curvelet transform in frequency domain. J. Appl. Geophys., 113: 64-73.

Zhang., C. and van der Baan, M., 2019. Strong random noise attenuation by shearlet transform and time-frequency peak filtering. Geophysics, 84(6): V319-V331.

Zwartjes., P.M. and Sacchi, M.D., 2007. Fourier reconstruction of nonuniformly sampled, aliased seismic data. Geophysics., 72(1): V21-V32.